



FULL-SCALE STATIC LOADING TEST ON A FIVE STORY REINFORCED CONCRETE BUILDING (Part2: Damage Analysis)

M. Tani⁽¹⁾, T. Mukai⁽²⁾, T. Demizu⁽³⁾, S. Kono⁽⁴⁾, H. Kinugasa⁽⁵⁾ and M. Maeda⁽⁶⁾

⁽¹⁾ Associate Professor, Kyoto University, tani@archi.kyoto-u.ac.jp

⁽²⁾ Senior Research Engineer, Building Research Institute, t_mukai@kenken.go.jp

⁽³⁾ Lecturer (Part-time), Tokyo University of Science, a22528@rs.tus.ac.jp

⁽⁴⁾ Professor, Tokyo Institute of Technology, kono@serc.titech.ac.jp

⁽⁵⁾ Professor, Tokyo University of Science, kinu@rs.noda.tus.ac.jp

⁽⁶⁾ Professor, Tohoku University, maeda@archi.tohoku.ac.jp

Abstract

Damage analysis was conducted on the static loading test data of the full-scale five-story reinforced concrete building utilizing wing walls for damage reduction. In experiment, damage was measured quantitatively for one beam with spandrel walls, two columns with wing walls, and one floor slab by recording width and length of all cracks and concrete spalling area at each peak and unloaded condition. After loading test, damage of these members was classified using the Japanese guideline (Guideline for post-earthquake damage evaluation and rehabilitation) based on recorded quantities. This damage analysis shows the effectiveness of structural slits for walls because the residual crack widths of the beam was as small as 0.2 mm or smaller. However, the damage class of beam became severe since the beam had a few large residual cracks. On the other hand, damage of wing walls was severer than damage of column, and it became clear that their damage should be evaluated individually. Then, the post-earthquake damage evaluation for the whole building was performed and the damage level of the building was "Moderate" or "Heavy" at 1/200 rad and 1/100 rad drift, respectively, while the building still had not reached the peak load. This shows that the current guideline is not able to evaluate the damage level of the building appropriately. The criteria of building function continuity proposed by authors were verified by comparison with the obtained experimental data. The guidelines use the maximum residual crack width and the degree of concrete crushing to classify the damage level of members. However, overall damage states such as the number and length of cracks and area of spalling and crushing of concrete needs to be evaluated for a proper and precise damage evaluation.

Keywords: Reinforced concrete; Full-scale test; Damage quantity measurement

1. Introduction

Continued functionality after earthquake and necessity of repair or/and retrofit for long-term use of damaged buildings are evaluated based on the damage condition. One of authors developed a database for repairable and post-earthquake functionality evaluation which can evaluate damage and reparability of R/C building according to the magnitude of seismic response [1]. The database includes detail damage information about the quantity of damage such as crack width, crack length and concrete spalling area. Authors have also conducted several series of experiments on R/C members with detail damage investigation to develop this database [2, 3], however, the amount of accumulated experimental data is not enough. Therefore, damage was measured quantitatively in detail for some members mainly on the first floor of the full-scale five-story R/C building specimen which was reported in part 1. The obtained damage data from the full-scale test is irrelevant to scale effect and invaluable for development of the database. Damage analysis was conducted on the members with detail damage measurement. The results of building damage rating using “the Guideline for post-earthquake damage evaluation and rehabilitation” [4] published by the Japan Building Disaster Prevention Association is also reported in this paper.

2. Outlines of Damage Measurement

2.1 Measurement procedures

Damage measurement in this experiment consisted of “detail measurement” and “normal measurement.” Detail measurement items were crack width, crack length and concrete spalling area. Crack width measurement was performed at each peak and unloaded condition during the second negative loading cycle (the first cycle for $R=1/1600$ rad and $1/800$ rad, R : total drift angle on roof level) for all visible cracks by using crack scale with 0.05 mm intervals. The maximum width of every visible crack was recorded. If two distinct cracks connected to one crack, they were treated as one crack. In the case that one crack branched off or met at the middle of another crack, they were considered as two distinct cracks. For crack pattern diagrams, residual visible cracks were recorded by tracing on the transparent films lapped over the surface of specimens at unloaded condition of the second negative loading cycle (the first cycle for $R=1/1600$ rad and $1/800$ rad). Dimension of concrete spalling was also recorded in the same manner. Crack diagrams and dimension of concrete spalling recorded on

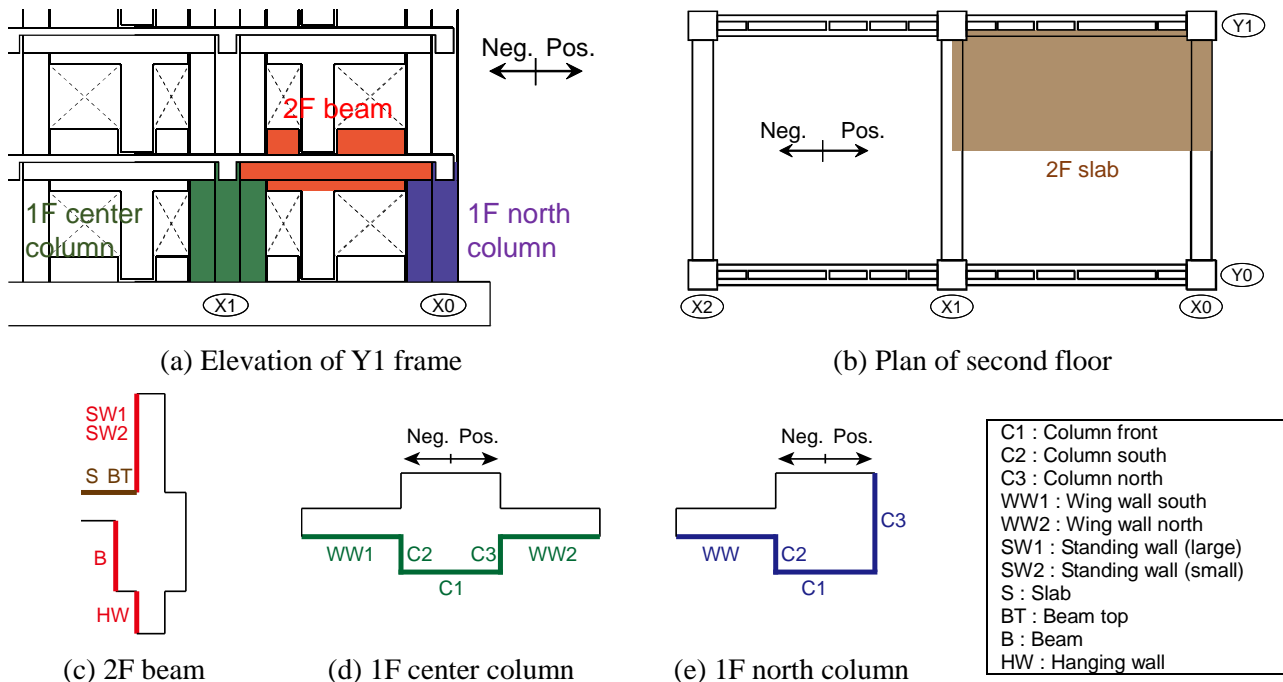


Fig. 1 – Regions for detail damage measurement



transparent films were converted into electronic data by using CAD software. Then crack length and concrete spalling area were calculated. Region for detail measurement was divided into many zones, and one person was in charge of detail measurement on assigned zone throughout the loading test to obtain consistent data. For normal measurement, the maximum crack width of each member was measured at each peak and unloaded condition, and crack pattern was recorded at each peak during the second negative loading (the first cycle for $R=1/1600$ rad and $1/800$ rad).

2.2 Regions for damage measurement

Regions for damage measurement are shown in Fig.1. Detail measurement was performed mainly for members of north-west span on the first floor. Damage was measured for interior faces of the second floor beam with spandrel walls, the first floor center column with wing walls (X1-Y1), the first floor north column with a wing wall (X0-Y1) and second floor slab (hereinafter abbreviated to “2F beam”, “1F center column”, “1F north column” and “2F slab”, respectively). Measuring region of 2F beam were divided into beam, hanging wall and two standing walls. Measuring region of 1F center and north columns was divided into three faces of column and wing walls. Measurement for bottom face of beam and side faces of walls were omitted. Damage measurement region of 2F slab was a north-west part, 6000 mm in longitudinal direction by 3000 mm in transverse direction, which corresponds to one-fourth of the total second floor area. Normal measurement was conducted from inside of the building for all columns and beams in all floors of west Y1 frame.

3. Results of Detail Damage Measurement

Results of detail damage measurement such as residual crack diagram, maximum crack width, residual crack length and concrete spalling area are shown in this chapter.

3.1 Residual crack diagram

Figure 2 illustrates crack pattern diagrams at unloaded condition during the second cycle of $R=1/50$ rad in which the maximum horizontal capacity was shown. Blue and red lines show the cracks appeared in positive and negative loading, respectively. Black lines indicate the cracks occurred before lateral loading.

2F beam: Beam damage was localized around the structural slits, and only minor damage was observed in the middle of beam. Spandrel walls are supposed to contribute to increasing beam stiffness because many cracks developed to the spandrel walls as shown in Fig. 2. Some cracks in the middle of hanging wall occurred because deep hanging wall touched to standing walls on the first floor during $R=1/50$ rad cycle.

1F center column: Flexural cracks occurred in wing walls and developed into column with increasing the number of cracks as lateral drift increased. Appearance of crack and concrete spalling was almost horizontally symmetric in positive and negative loading. Cover and core concrete spalling of wing walls were observed during $R=1/100$ rad and $R=1/67$ rad cycles, respectively. Vertical rebars in boundary element of wing wall

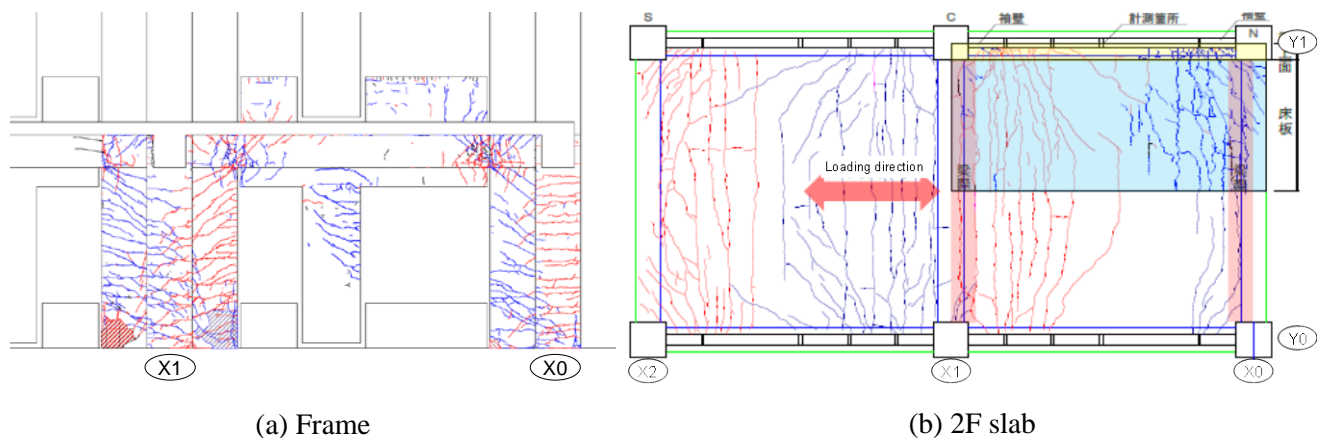


Fig. 2 – Residual crack diagram ($R=1/50$ rad)



fractured during $R=1/50$ rad cycle.

1F north column: In negative loading, axial tensile force applied to the north columns because of overturning moment, and column located on tension side of the member. Therefore, flexural cracks appeared uniformly over the whole length of column. It is supposed that whole column cross-section was tensile stressed. In positive loading, not only flexural cracks but shear cracks which develop to column base occurred. Reinforcement was not exposed while moderate cover concrete spalling at wing wall edge was observed during the final loading cycle.

2F slab: During $R=1/1600$ rad cycle, some flexural cracks on beam top face occurred from wing wall edge. Then, these cracks developed diagonally during $R=1/800$ rad cycle. After that, new cracks occurred near longitudinal beam and developed to transverse direction straightly. Even after $R=1/50$ rad cycle, the damage around the center of slab was slight compared to the damage near beams. Most cracks which occurred from wing wall edges near X1 frame oriented to transverse direction straightly, while many cracks near X0 frame developed diagonally from wing wall edges. In the past experiment [5], flexural cracks of slab developed from longitudinal beam to transverse direction straightly. It is supposed that the existence of wing walls affected to the crack development.

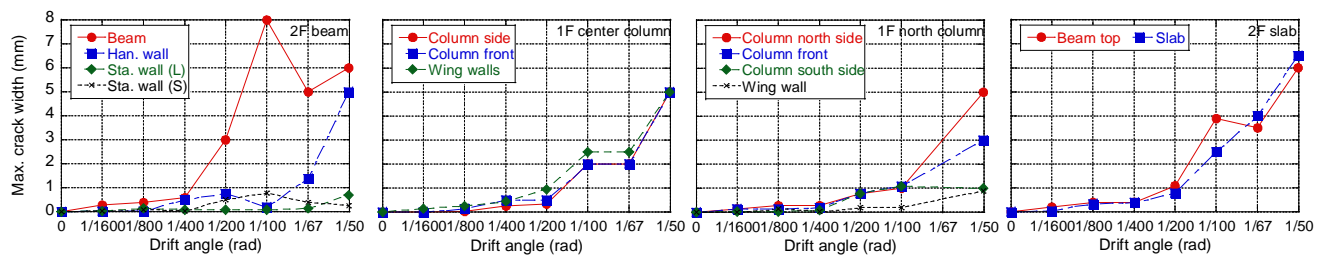
3.2 Maximum crack width

Maximum crack widths during each loading cycle at each peak and unloaded condition are shown in Fig. 3.

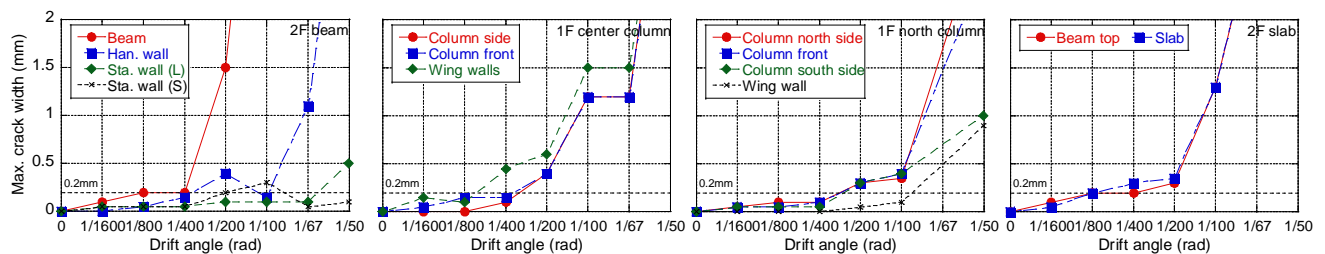
2F beam: Maximum crack widths at each peak and unloaded condition increased much during $R=1/200$ rad cycle as shown in Fig. 3. A few cracks near structural slit opened significantly due to yielding of beam main rebar near structural slit during $R=1/200$ rad cycle. Maximum residual crack width of beam reached to 5.0 mm during $R=1/100$ rad cycle. Maximum crack widths of spandrell walls were smaller than those of beams.

1F center column: Some difference between maximum crack width of column front face and column side faces was observed during small drift. However, crack width of column side faces became almost equal to that of column front face after $R=1/100$ rad cycle because the cracks of column front face connected to those of column side face as lateral deformation progressed. Maximum crack width of wing walls was relatively smaller than that of column as shown in Fig. 3.

1F north column: Column front face and north side face were located in tension side of member. Therefore, crack widths of them were relatively larger at peak, while crack widths of three faces of column



(a) At peak displacement



(b) After unloading

Fig. 3 – Maximum crack width



became close to each other at unloaded condition till $R=1/100$ rad cycle. During $R=1/50$ rad cycle in which column tensile rebars yielded, crack widths of column front face and north side face increased much and maximum residual crack width exceeded 2.0 mm. Maximum crack width of wing wall was relatively smaller than that of column because wing wall located in compression side of member during negative loading.

2F slab: Maximum crack width at peak and unloaded condition increased significantly during $R=1/100$ rad cycle due to slab reinforcement yielding. Observed maximum crack widths of beam top face and slab at peak were 3.9 mm and 2.5 mm, respectively. Residual maximum crack widths of both beam top face and slab were 1.3 mm. Flexural cracks were dominant among the damage of slab. Maximum residual crack width was nearly half of the width at peak till $R=1/200$ rad cycle in which slab reinforcement was still elastic. The same tendency was observed after slab reinforcement yielding except $R=1/67$ rad cycle. Obvious difference between the crack widths of beam upper face and slab was not seen in terms of changes of maximum crack widths as shown in Fig. 3.

3.3 Residual crack length

“Crack length ratio” is defined as an index for unit quantity of crack length for comparison of damage amount between different members. Crack length ratio is calculated by dividing crack length by the square root of measuring region area. The reason why crack length was divided by the square root of measuring region area instead of measuring region area is to eliminate scale effect. Residual crack length ratio at each drift is shown in Fig.4. In this figure, cracks are classified into five categories by residual crack width W_r ($W_r < 0.2$ mm, 0.2 mm $\leq W_r < 1.0$ mm, 1.0 mm $\leq W_r < 2.0$ mm, 2.0 mm $\leq W_r < 5.0$ mm, 5.0 mm $\leq W_r$).

2F beam: Total crack length of all parts (beam, hanging wall and spandrel walls) increased monotonically. In the case of beam, crack length of $W_r \geq 0.2$ mm (repair is required) constituted 6.5 % of the total crack length

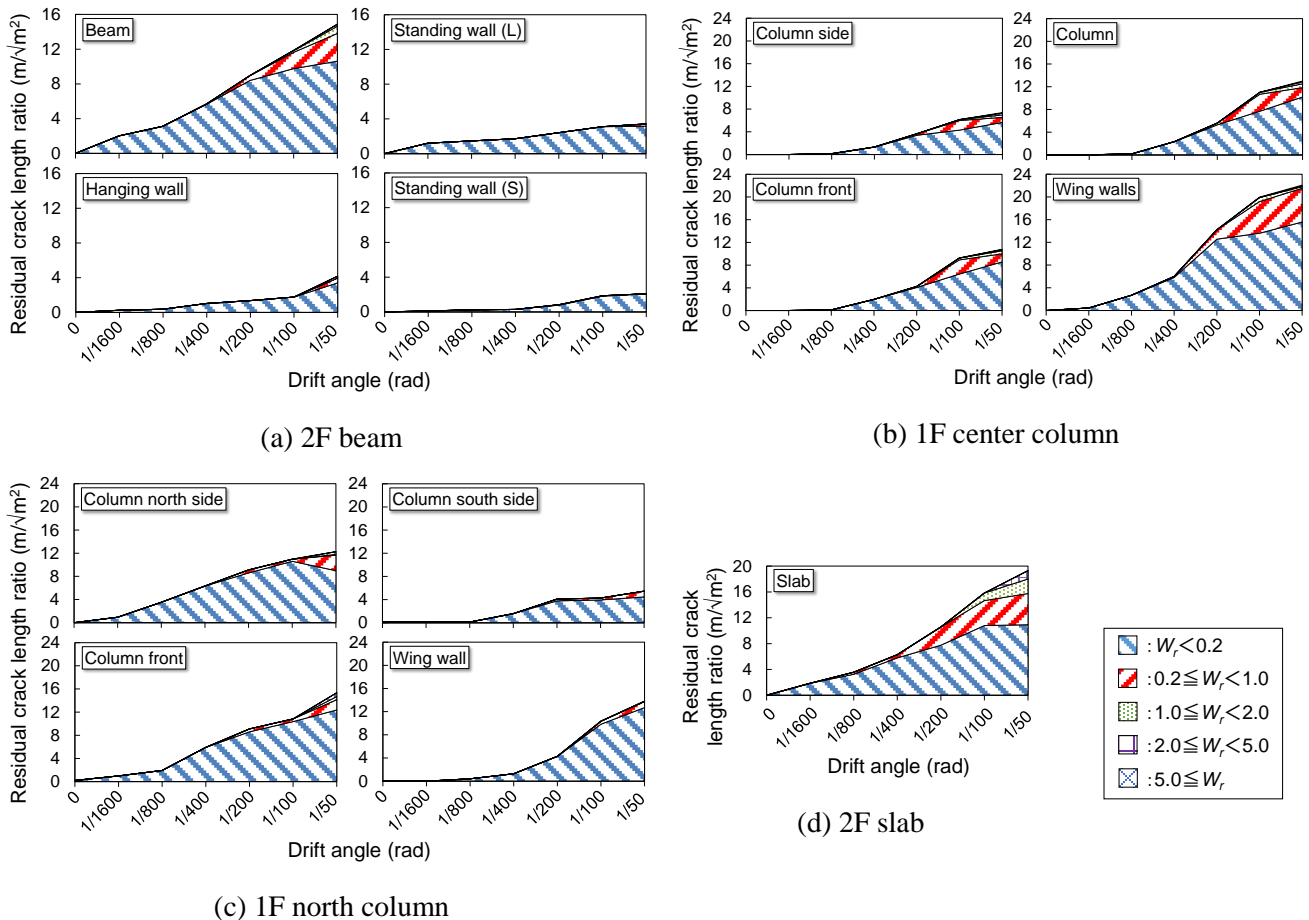


Fig. 4 – Residual crack length ratio



at $R=1/200$ rad cycle. Then, increment of crack length of $W_r < 0.2$ mm (repair is not necessary) slowed and crack length of $W_r \geq 0.2$ mm increased. However, Fig.4 (a) shows that cracks of $W_r < 0.2$ mm were dominant. It indicated that structural slits lead concentration of deformation to a few cracks near structural slits. Most cracks of spandrel walls were slight as their widths were less than 0.2 mm because of structural slits, as seen in beam.

1F center column: Crack length ratio of wing walls was slightly larger than those of three column faces when lateral drift was small. After $R=1/100$ rad cycle, the difference between crack length ratios of wing walls and column became large. Crack length ratio of column front face was 1.2 times larger than that of column side face at $R=1/50$ rad cycle. Most cracks of column and wing walls were slight cracks ($W_r < 0.2$ mm) till $R=1/200$ rad cycle. After that, crack length of $W_r \geq 0.2$ mm increased significantly.

1F north column: The trends of crack length ratio of column front face and column south side face became similar, because obvious difference between crack appearance of them was not observed as shown in Fig. 2. Crack length ratio in column front face increased from small drift angle, and crack length ratio of $W_r \geq 0.2$ mm in column front face was larger compared to that of wing wall. In the case of wing wall, crack length ratio of $W_r \geq 0.2$ mm started increasing after $R=1/400$ rad cycle.

2F slab: Total crack length increased monotonically. Cracks of $W_r \geq 0.2$ mm were hardly observed till $R=1/400$ rad cycle. During $R=1/200$ rad cycle, crack length of $W_r \geq 0.2$ mm started increasing. Crack length of $W_r \geq 1.0$ mm increased after $R=1/100$ rad cycle in which slab reinforcement yielded. At $R=1/50$ rad cycle, crack length of $W_r \geq 0.2$ mm constituted 43 % of the total crack length.

3.4 Concrete spalling area

“Spalling area ratio” is defined as an index for unit quantity of concrete spalling area. Spalling area ratio is calculated by dividing spalling area by measuring region area. Spalling area ratio at each loading cycle after unloading is shown in Fig. 5.

2F beam: Concrete spalling of beam was slight as cover and core concrete spalling ratios were 1.47 % and 0.036 %, respectively. Some cover concrete spalling of hanging wall was observed near structural slits at $R=1/50$ rad cycle. Cover concrete spalling of standing walls was very slight compared to that of hanging wall. Core concrete of spandrel walls did not spall.

1F center column: Concrete spalling of column was very slight while concrete spalling of wing walls became significant after $R=1/100$ rad cycle. Difference between concrete spalling ratios of north and south wing walls was not small ($> 100 \text{ cm}^2/\text{m}^2$). Therefore, detail analysis on applied force and moment is needed. Spalling ratio of core concrete rapidly increased during $R=1/50$ rad cycle.

1F north column: Spalling ratio of column started to increase from $R=1/100$ rad cycle. Spalling ratio of

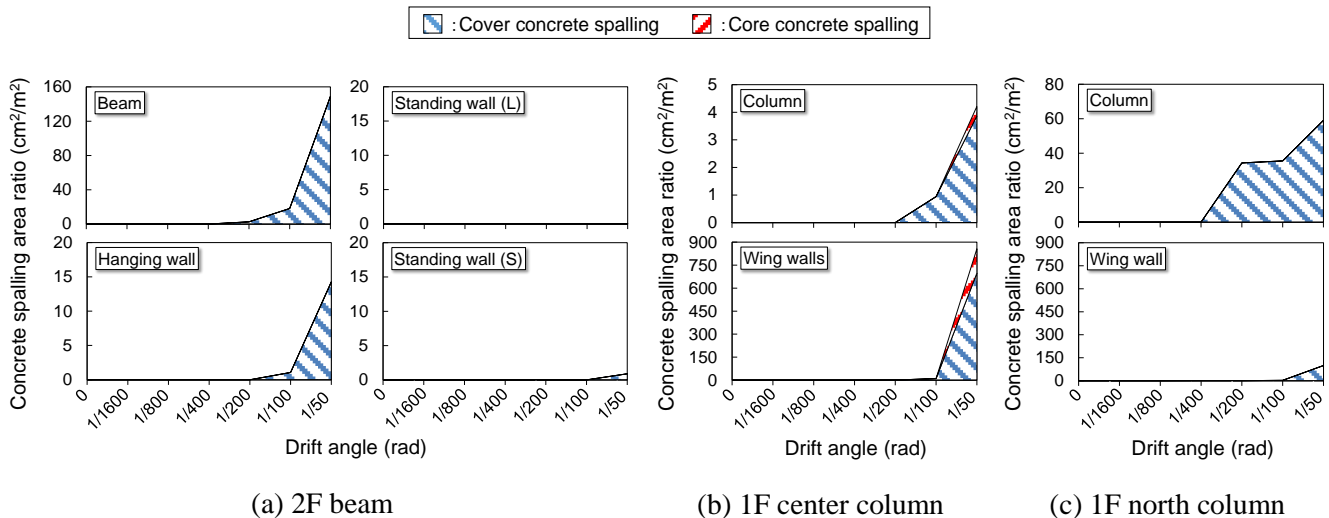


Fig. 5 – Concrete spalling area ratio



wing wall rapidly increased at $R=1/50$ rad cycle because of concrete crushing at the wall edge. Core concrete spalling was not observed till the final loading cycle.

2F slab: No concrete spalling was observed till $R=1/67$ rad cycle. Slight spalling of cover concrete which corresponds to spalling area ratio of 0.0019 % occurred at the corners near columns during $R=1/50$ rad cycle.

3.5 Damage class

In Japan, “Guideline for Post-earthquake Damage Evaluation and Rehabilitation” published by the Japan Building Disaster Prevention Association [4] is commonly used for residual seismic capacity evaluation of earthquake-affected buildings. First of all, damage classification of structural members is performed based on the damage definition shown in Table 1. Structural members are classified into one of five categories I through V. Next, residual capacity of each member is calculated considering seismic capacity reduction factor η which corresponds to damage class. Finally, residual seismic capacity of story is evaluated based on residual capacity of each member.

Table 1 – Definition of Damage class for R/C members [4]

Damage class	Description of damage	Residual capacity reduction factor η	
		Ductile column	Other members
I	Visible narrow cracks on concrete surface (Crack width is less than or equal to 0.2mm)	0.95	0.95
II	Visible clear cracks on concrete surface (Crack width is about 0.2-1.0mm)	0.75	0.6
III	Local crush of cover concrete, Remarkable wide cracks (Crack width is about 1.0-2.0mm)	0.5	0.3
IV	Remarkable crush of concrete with exposed reinforcing bars, Spalling off of cover concrete (Crack width is more than 2.0mm)	0.1	0
V	Buckling of reinforcing bars, Cracks in core concrete, Visible vertical and/or lateral deformation in columns and/or walls, Visible settlement and/or inclination of the building	0	0

Table 2 – Damage classes

Drift angle	2F beam				1F center column		1F north column		2F slab	
	B	HW	SW1	SW2	C	WW	C	WW	BT	S
1/1600	I	I	I	I	I	I	I	I	I	I
1/800										
1/400		III		III	III	III				
1/200	IV		III				II	II	III	III
1/100		IV		III	II	III				
1/67	IV		IV				II	V	V	-
1/50		IV		IV	II	V				V

B: Beam, HW: Hanging wall, SW1: Standing wall (large), SW2: Standing wall (small), C: Column, WW: Wing wall, BT: Beam top face, S: Slab



Results of damage classification for each member are shown in Table 2. Damage classification was performed for column, beam and wall in this study considering damage condition of each part was quite different, although damage class of column or beam with wall is given as one member in common. For damage classification of floor slab, the method for column and beam shown in Ref. [4] was applied in this study because criterion for damage classification of slab is not specified.

2F beam: Damage class was tended to be determined by crack width in the case that core concrete spalling is slight because damage concentrates to a few cracks near structural slit as seen in the experiment. At $R=1/100$ rad cycle, damage class was judged as IV because some cracks significantly opened near structural slits.

1F center column: Damage class of column was determined by crack width till $R=1/200$ rad cycle because concrete spalling was not observed. At $R=1/50$ rad cycle, damage class was judged as V due to core concrete spalling at column base. Damage class of wing walls was determined by crack width till $R=1/100$ rad cycle because concrete spalling was hardly observed. Then, core concrete spalling at wing wall base lead damage class V at $R=1/67$ rad cycle. Although the horizontal load carrying capacity of column with wing walls might be deteriorated, the member is considered to be repairable because it is supposed that column had enough horizontal and vertical load carrying capacity. After $R=1/50$ rad cycle, core concrete spalling of wing walls progressed and vertical rebar of wing wall fractured at wall base.

1F north column: As observed damage was slight till $R=1/100$ rad cycle, damage classes of column and wing wall were less than II and I, respectively. Damage class of column increased to IV at $R=1/50$ rad cycle. Damage class of wing wall was III with conservative evaluation considering cover concrete spalling, while judgement by maximum residual crack width gave damage class II. It is assumed that enough seismic capacity was assumed to remain and the damage was repairable.

2F slab: Damage class of slab was determined by crack width because concrete spalling was hardly observed as shown in the previous section. Results of damage classification of beam top face and slab were almost the same because changes of maximum crack width of them also showed the same tendency. Damage class of beam top face was equal to or smaller than that of beam during all loading cycle.

4. Building Damage Rating

4.1 Outline of building damage rating

Damage classification of each member and damage rating of whole building were performed based on Ref [4]. Damage classification was performed for columns with wing walls and beams in Y1 frame (longitudinal direction) considering measured maximum residual crack width and concrete spalling. Damage class of column with wing wall was determined as the larger of the damage classes of column and wing wall. Residual crack width of slab was not considered in the damage classification. Damage rating was also performed for Y1 frame based on the results of damage classification. Residual seismic capacity ratio was calculated based on the simplified procedure shown in Ref [4] by considering seismic capacity reduction factor η for ductile column and the assumption that each column has the same strength. In the case damage class of beams judged by considering residual crack width measured below slab was larger than damage class of column connecting to them, damage class of beam was read as that of column [4].

4.2 Results of building damage rating

Damage classes of columns with wing walls and beams in Y1 frame at each loading cycle are shown in Fig. 6. As shown in Fig. 6, many beams showed much larger damage class than columns connected to the beams. Beam deformation was concentrated to a few cracks because of the structural slits at beam ends as described above. Consequently, the evaluated damage classes of beams became larger. There was not much difference between damage classes of columns and beams (0 or I) till $R=1/400$ rad cycle. Damage classes of beams increased precedingly to those of columns except first floor column after $R=1/200$ rad cycle.

Residual seismic capacity ratio and damage rate of each floor are shown in Fig. 7 and Table 3, respectively. Residual seismic capacity ratio and damage rate of first floor during $R=1/67$ rad cycle are shown as

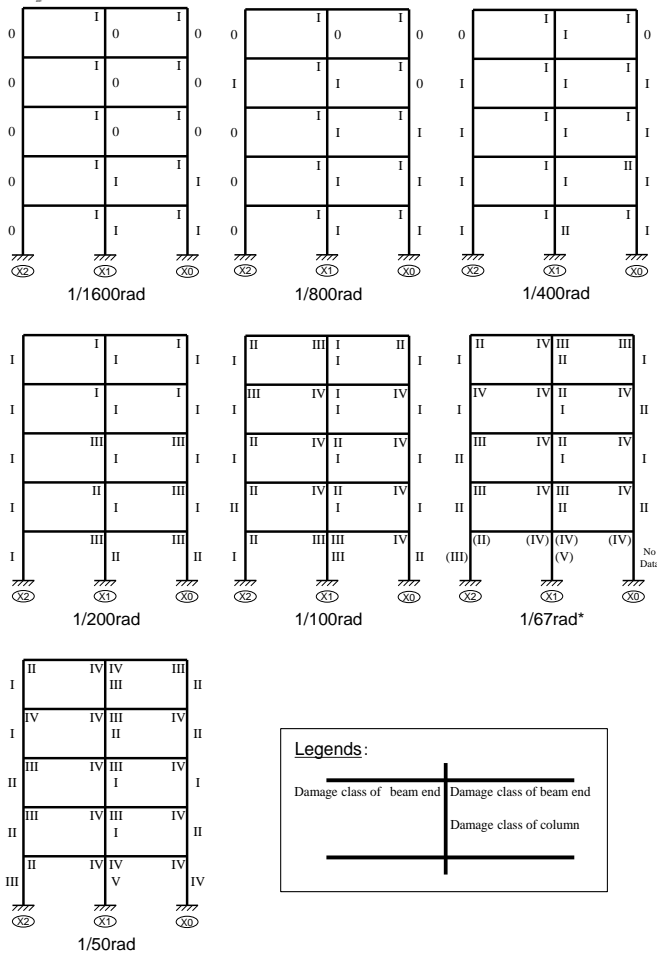


Fig. 6 – Damage class of each member

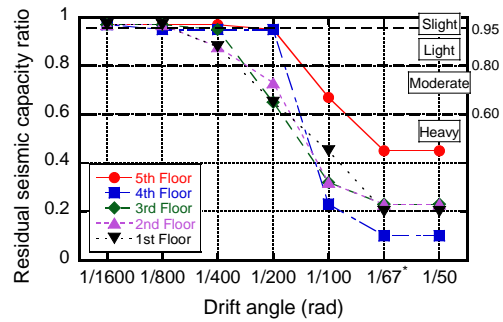


Fig. 7 – Residual seismic capacity ratio

Table 3 – Damage rate of each floor

Drift angle	5th floor	4th floor	3rd floor	2nd floor	1st floor
1/1600	Slight	Slight	Slight	Slight	Slight
1/800				Light	Light
1/400			Moderate	Moderate	Moderate
1/200	Heavy	Heavy	Heavy	Heavy	Heavy
1/100					
1/67*					
1/50					

a reference with “*”, because other person observed crack width and column with wing wall in X0 frame was unmeasured and estimated to be IV considering the damage during of previous and next loading cycle. As shown in Fig. 7 and Table 3, damage rates of all floor were “Slight” till $R=1/800$ rad cycle. Then, damage rate increased in order from lower floor as lateral loading progressed. Maximum damage rate was “Light” during $R=1/400$ rad cycle, “Moderate” during $R=1/200$ rad cycle, and “Heavy” after $R=1/100$ rad cycle. After $R=1/67$ rad cycle, all floors were rated as “Heavy”. Because this specimen was designed as beam-hinging mechanism, formation of plastic beam hinge over the entire building led larger damage rate even in upper floor.

The building had not reached the peak load during $R=1/200$ rad and $1/100$ rad cycles in which damage rates were moderate and severe. Therefore, current damage rating method [4] turned out to give too conservative estimation. This result indicates that detail discussion on building functionality evaluation is needed in the case that a few cracks open significantly and damage classes of structural members are tend to be determined by maximum residual crack widths, even current method permits to apply the damage classification criteria of column and structural wall for beam.

4.3 Discussion on post-earthquake functional-use

Authors proposed an evaluation method of post-earthquake functional-use in Ref. [6]. Ranking of damage state of R/C superstructure is listed in Table 4. Relationship between damage rank and target grade of post-earthquake functional-use which is proposed for superstructure is shown in Table 5. Target grade of post-earthquake functional-use consists of three grades “S”, “A” and “B”, correspond to target level of restriction of building



Table 4 – Ranking of damage state of R/C superstructure [6]

Ranking of damage state		Damage state of R/C super structure
I	Damage (except slight damage needs not emergency countermeasure) is not allowed after large earthquake.	S_{R-I} : Enough high residual seismic capacity is secured while no repair is needed due to damage on structural members. (ex. Residual crack width is less than 0.2 mm)
II	Implementation of emergency countermeasure or minor repair on the minor damage is allowed after large earthquake.	S_{R-II} : Enough high residual seismic capacity is secured while quick recovery is not needed due to damage on structural members. (ex. Residual crack width is less than 1.0 mm, corresponds to damage class II)
III	Implementation of emergency countermeasure or repair on the damage is allowed after large earthquake.	S_{R-III} : Moderate residual seismic capacity is secured while damage on structural members should be repaired according to appropriate plan. (ex. Residual crack width is less than 2.0 mm, corresponds to damage class III)

Table 5 – Relations between target grades of post-earthquake functional-use and damage rank [6]

Target grades of post-earthquake functional-use		Damage rank of R/C superstructure
S	Functionality of the building is secured without any restriction of use in whole building.	S_{R-I} S_{R-II} S_{R-III}
A	Functionality of important area is secured with restriction of use in a part of building	
B	Functionality is secured after a certain countermeasure while functional-use is restricted in a part of building including important area.	

usage. Grade S is associated with damage rank of S_{R-I} which doesn't allow any damage except for slight damage needs not emergency countermeasure. Partial damage is allowed gradually for grade A and B.

The post-earthquake functional-use of the five-story specimen is discussed based on the evaluation method shown in Ref. [6]. At $R=1/1600$ rad cycle, the maximum residual crack width of each member was less than 0.2 mm (damage rank S_{R-I}). This result means that the building is regarded as grade S if the seismic response can be kept within $R=1/1600$ rad. At $R=1/800$ rad and $1/400$ rad cycles, the maximum residual crack width of a few members exceeded 0.2 mm (damage rank S_{R-II}), that corresponds to grade A. At $R=1/200$ rad cycle, the damage ranks of stories from first floor to third floor became S_{R-III} . If the target grade was set to grade B, the seismic response of $R=1/200$ rad is allowable. After $R=1/100$ rad, complying the criteria of target grade B was difficult due to severe damage of all stories. As described above, the lower damage rank and target grade evaluation was given based on the criteria of the maximum residual crack width as shown in the Guidelines because of widely opened cracks due to the existence of structural slits. Therefore, a further discussion on the criteria considering reparability such as the number of widely opened cracks is needed.

5. Conclusions

Damage analysis and building damage rating by the Japanese Guideline were performed on the full-scale five-story R/C building specimen. Obtained findings are listed below.

- A few cracks on beams near structural slits opened significantly. As a result, damage class is tended to be determined by residual crack width. Most cracks of spandrel walls were slight as their widths were less than 0.2 mm (repair is not needed) because of structural slits

- Columns with wing walls showed different tendency in damage progress and damage amount of column and wing walls. Concrete spalling area ratio of wing walls was extremely larger than that of column in the case



of 1F middle column. 1F north column was located in tension side when wing wall was compressed during the negative loading. As a result, the damage of column was larger than that of wing wall in terms of residual crack length ratio and concrete spalling area ratio. These results indicate that the damage of column and wing walls should be evaluated separately.

- Many beams showed much larger damage class than columns connected to the beams. Till $R=1/400$ rad cycle, there was not much difference between damage classes of columns and beams (0 or I). Damage classes of beams increased precedingly to those of columns except first floor column after $R=1/200$ rad cycle. Current damage rating method turned out to give too conservative estimation. This result indicates that detail discussion on evaluation of building functionality is needed in the case that a few cracks open significantly and damage classes of structural members are tend to be determined by maximum residual crack widths, even current method permits to apply the damage classification criteria of column and structural wall for beam.

- The specimen complied the criteria of target grade S in terms of the evaluation method of post-earthquake functional-use proposed by authors after $R=1/1600$ rad, grade A after $R=1/800$ rad and $R=1/400$ rad, and grade B after $R=1/200$ rad, respectively. The target grade was determined by the damage of beam in all cases.

6. Acknowledgements

This experiment was conducted by the research project of National Institute for Land and Infrastructure Management “Development of function sustaining technologies for buildings used as Disaster Prevention Bases.” The discussion in this paper is based on the experimental data obtained through the collaboration research with the research project of Building Research Institute “Development on Seismic Design Method for Building with Post-Earthquake Functional Use.” The static loading test was carried out by structural engineers of Nishimatsu Construction Co. Ltd., Hazama Ando Corporation, Kumagai Gumi, Sato Kogyo Co. Ltd, Toda Corporation, Fujita Corporation, and Maeda Corporation. Damage measurement was conducted with great assistance by Dr. Hidekazu Watanabe, Assistant Professor of Tokyo Institute of Technology, and the students of Kono Laboratory in Tokyo Institute of Technology, Kinugasa Laboratory in Tokyo University of Science and Maeda Laboratory in Tohoku University.

7. References

- [1] Mukai T, Fukuyama H, Morita K, Saito T, Kato H (2011): Proceedings of Development on New Structural Performance Evaluation System for Disaster Resilient Buildings. *BRI Proceedings*, **20**, Building Research Institute, Tsukuba, Japan. (in Japanese)
- [2] Tani M, Mukai T, Ogura M, Taleb R, Kono S (2014): Full-scale Experiment on Non-structural R/C Walls Focused on Failure Modes and Damage Mitigation. *Second European Conference on Earthquake Engineering and Seismology*, ID 656, Istanbul, Turkey.
- [3] Fukuyama H, et al. (2011): Experimental test on structural performance for RC frame with brittle column. *Summaries of Technical Papers of Annual Meeting*, Architectural Institute of Japan, 807-822. (in Japanese)
- [4] Nakano Y, Maeda M, Kuramoto H, Murakami M (2003): Guideline for post-earthquake damage evaluation and rehabilitation of RC buildings in Japan. *Proceedings of the 2nd Korea-Japan Workshop on New Direction for Enhancement of Structural Performance - Formulation, Verification, and Its Application -*, 4-1-4-17, Yokohama, Japan.
- [5] Kaminosono T, Yoshimura M, Okamoto S, Nakata S (1987): Pseudo-dynamic test of full-scale reinforced concrete seven-story structure. *Journal of Structural and Construction Engineering*, Architectural Institute of Japan, **377**, 64-72. (in Japanese)
- [6] Kikitsu H, Mukai T, Kato H, Hirade T, Hasegawa T, Tani M, Kashiwa H, Iiba M (2015): Structural design and seismic performance evaluation for new buildings with post-EQ functional-use (Part 1 Outline of performance required for post-EQ functional-use), *Summaries of Technical Papers of Annual Meeting*, Architectural Institute of Japan, 45-46. (in Japanese)